

Induction of human neuronal cells by defined transcription factors

Zhiping P. Pang^{1*}, Nan Yang^{2*}, Thomas Vierbuchen^{2,3*}, Austin Ostermeier^{2,3}, Daniel R. Fuentes², Troy Q. Yang², Ami Citri⁴, Vittorio Sebastiano², Samuele Marro², Thomas C. Südhof^{1,5} & Marius Wernig^{2,3}

Somatic cell nuclear transfer, cell fusion, or expression of lineage-specific factors have been shown to induce cell-fate changes in diverse somatic cell types^{1–12}. We recently observed that forced expression of a combination of three transcription factors, *Brn2* (also known as *Pou3f2*), *Ascl1* and *Myt1l*, can efficiently convert mouse fibroblasts into functional induced neuronal (iN) cells¹³. Here we show that the same three factors can generate functional neurons from human pluripotent stem cells as early as 6 days after transgene activation. When combined with the basic helix–loop–helix transcription factor *NeuroD1*, these factors could also convert fetal and postnatal human fibroblasts into iN cells showing typical neuronal morphologies and expressing multiple neuronal markers, even after downregulation of the exogenous transcription factors. Importantly, the vast majority of human iN cells were able to generate action potentials and many matured to receive synaptic contacts when co-cultured with primary mouse cortical neurons. Our data demonstrate that non-neural human somatic cells, as well as pluripotent stem cells, can be converted directly into neurons by lineage-determining transcription factors. These methods may facilitate robust generation of patient-specific human neurons for *in vitro* disease modelling or future applications in regenerative medicine.

Encouraged by our recent findings in mouse cells¹³, we explored in this study whether human fibroblasts could also be directly induced to become functional neurons. This was unclear given the differences in the gene regulatory networks governing human and rodent neural development^{14–16}. First, we sought to determine whether forced expression of transcription factors could induce a neuronal fate in human pluripotent cells. To that end, we infected undifferentiated human embryonic stem (ES) cells in chemically defined N3 media¹⁷ with *Brn2*, *Ascl1* and *Myt1l* (BAM) using doxycycline (dox)-inducible lentiviral vectors together with an EGFP (enhanced green fluorescent protein) virus. The majority of ES cells were EGFP-positive 24 h after addition of doxycycline (Supplementary Fig. 1). Strikingly, as early as 3 days after doxycycline treatment, we observed bipolar neuron-like cells surrounding nearly all ES cell colonies (Fig. 1a and Supplementary Fig. 1). By day 8, cells with more mature neuronal morphologies that expressed both β -III-tubulin (Tuj1, also known as TUBB3) and MAP2 had migrated away from ES cell colonies and were present throughout the plate (Fig. 1b, c). In contrast, after infection with EGFP virus alone, no neuronal cells were generated during the same timeframe, and nearly all ES cells had died due to the cytosine β -D-arabino-furanoside (Ara-C) treatment. We then determined the relative contribution of the three factors and found that *Ascl1* alone was sufficient to induce MAP2-positive cells (Supplementary Fig. 2). The addition of *Brn2* or *Myt1l* or both did not increase the efficiency of neuronal differentiation but induced more complex morphologies. Cells infected with all three factors together had the most mature neuronal morphologies

(Supplementary Fig. 2). Electrophysiological analysis surprisingly revealed that as early as 6 days after induction all recorded cells ($n = 16$) generated action potentials (Fig. 1d). At day 15 after doxycycline treatment, the average resting membrane potential of neuronal cells was -51 ± 1.8 mV (mean \pm s.e.m., $n = 18$) (Fig. 1f and Supplementary Table 1). These ES-iN cells exhibited prominent

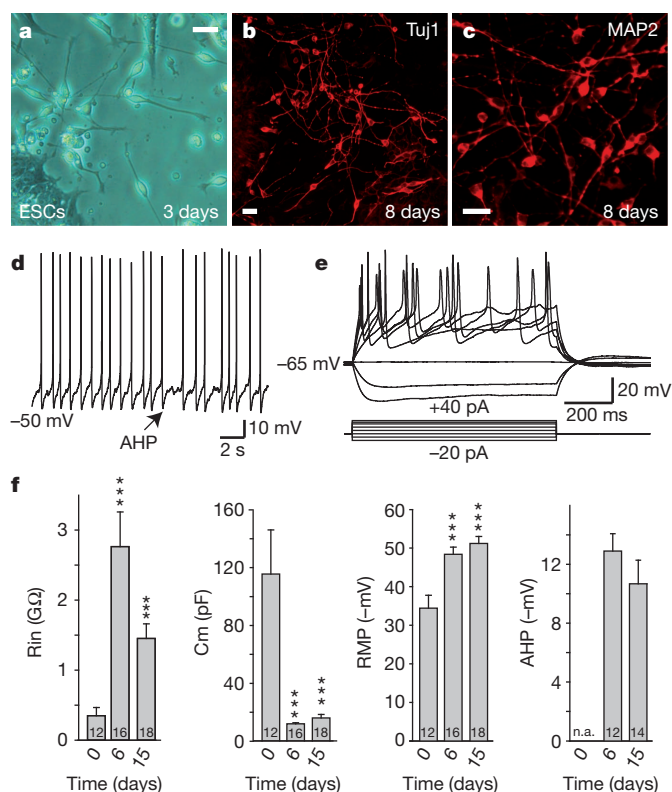


Figure 1 | Rapid generation of functional neurons from human ES cells.

a, Three days after induction, ES-iN cells showed bipolar neuronal morphologies. **b**, **c**, Eight days after induction, ES-iN cells expressed Tuj1 (**b**) and MAP2 (**c**). **d**, Spontaneous action potentials presumably caused by membrane potential fluctuations recorded from an ES-iN cell 6 days after induction. Arrow, pronounced after hyperpolarization potentials (AHP). **e**, Representative traces of action potentials in response to step current injections 15 days after induction. Membrane potential was maintained at approximately -63 mV. **f**, Quantification of intrinsic membrane properties in control ES cells (0 day) before and after viral transduction. Rin, membrane input resistance; RMP, resting membrane potential; Cm, capacitance. Scale bars, 10 μ m (**a**, **b**, **c**). Numbers of cells recorded are labelled in the bars. Note the heterogeneity of the parameters (see also Supplementary Fig. 1). Data are presented with mean \pm s.e.m. *** $P < 0.05$.

¹Department of Molecular and Cellular Physiology, Stanford University School of Medicine, 265 Campus Drive, Stanford, California 94305, USA. ²Institute for Stem Cell Biology and Regenerative Medicine, Department of Pathology, Stanford University School of Medicine, 265 Campus Drive, Stanford, California 94305, USA. ³Program in Cancer Biology, Stanford University School of Medicine, 265 Campus Drive, Stanford, California 94305, USA. ⁴Department of Psychiatry and Behavioral Sciences, Stanford University School of Medicine, 265 Campus Drive, Stanford, California 94305, USA. ⁵Howard Hughes Medical Institute, Stanford University School of Medicine, 265 Campus Drive, Stanford, California 94305, USA.

*These authors contributed equally to this work.

after-hyperpolarization potentials (AHPs) following action potentials (Fig. 1d, f). Similar findings could be observed when human induced pluripotent stem (iPS) cells were infected (Supplementary Fig. 3). Thus, the BAM factors rapidly induce neuronal differentiation of human pluripotent stem cells.

Next, we asked whether human fibroblasts could also be directly converted into neurons. To this end, we derived three independent primary human fetal fibroblast lines (HFFs) (see Methods) and performed an extensive characterization of these cultures in various growth conditions to confirm that they lack spontaneous neuronal differentiation potential and do not contain detectable amounts of neural crest stem cells (see Supplementary Fig. 4). Strikingly, 7–10 days after infection with the BAM factors we could detect cells with immature neuronal morphologies. These cells expressed Tuj1 (Supplementary Fig. 5a), but remained functionally immature as revealed by their inability to generate action potentials 20 days after doxycycline treatment (Supplementary Fig. 5b). Thus, the BAM factors seemed to induce neuronal features but were insufficient to generate functional neurons from human fetal fibroblasts under these conditions.

Therefore, we screened 20 additional factors that could improve the generation of neuronal cells in combination with the BAM pool. We observed that *NeuroD1*, another basic helix–loop–helix transcription factor, improved the efficiency of generating Tuj1-positive neuronal cells two to threefold after 3 weeks (Fig. 2a). To determine the relative contribution of *NeuroD1*, we tested various combinations of these four factors. *NeuroD1* alone had no effect, but surprisingly in combination with *Brn2* it was sufficient to generate a similar number of Tuj1-positive neuronal cells compared to the BAN (*Brn2*, *Ascl1* and *NeuroD1*), BMN (*Brn2*, *Myt1l* and *NeuroD1*) and BAMN (*Brn2*, *Ascl1*, *Myt1l* and *NeuroD1*) pools (Supplementary Fig. 6a). However, further morphological and functional characterization showed that the BAMN combination generated the most mature neuronal cells (Supplementary Fig. 6b). We therefore decided to focus the further analysis on BAMN-iN cells.

Two weeks after induction, BAMN-iN cells showed neuronal morphologies and were labelled with pan-neuronal antibodies such as anti-Tuj1, anti-NeuN (also known as Rbfox3), anti-PSA-NCAM (polysialylated neural cell adhesion molecule) and anti-MAP2 (Fig. 2b–f). After extended culture periods of 4–5 weeks, we could detect cells expressing neurofilaments (Supplementary Fig. 7a), and rare neuronal processes decorated with punctate staining of synapsin and synaptotagmin, two synaptic vesicle proteins (Fig. 2g, h and Supplementary Fig. 7b). To ensure the co-expression of pan-neuronal and subtype specific markers, we performed single-cell gene-expression profiling of iN cells using Fluidigm dynamic RT-PCR arrays¹⁸. We analysed 54 single HFF-iN cells 34 days after doxycycline treatment from two independently infected cultures (Supplementary Fig. 8). These data revealed robust co-expression of multiple pan-neuronal and synaptic markers in 50/54 HFF-iN cells (β -III-tubulin, *DCX*, *MAP2*, *NCAM*, synapsin). Over half (29 of 54) of the iN cells analysed expressed mRNAs typical for glutamatergic neurons, such as *vGLUT1*, *vGLUT2* (also known as *SLC17A7* and *SLC17A7*, respectively) or both (Fig. 2i). Only two iN cells expressed *GAD67* (also known as *Gad1*) in the absence of *vGLUT1* or 2, and no iN cell expressed the inhibitory marker gene *vGAT* (also known as *SLC32A1*). Five cells expressed the catecholaminergic neuron marker tyrosine hydroxylase. Immunofluorescence analysis revealed that 5 weeks after infection $17 \pm 8\%$ of iN cells expressed the forebrain marker *Tbr1*, $21 \pm 9\%$ expressed the marker of peripheral neurons peripherin, whereas *En1*, a marker of midbrain neurons, serotonin and choline acetyltransferase were not detectable (Supplementary Fig. 9).

To assess whether the iN cell state was stable without continued transgene expression, we monitored the mRNA expression levels of endogenous and exogenous BAMN genes before and after doxycycline induction and after doxycycline withdrawal. Whereas the exogenous transgenes were clearly doxycycline-dependent, the four corresponding endogenous genes were rapidly induced and exhibited increasing

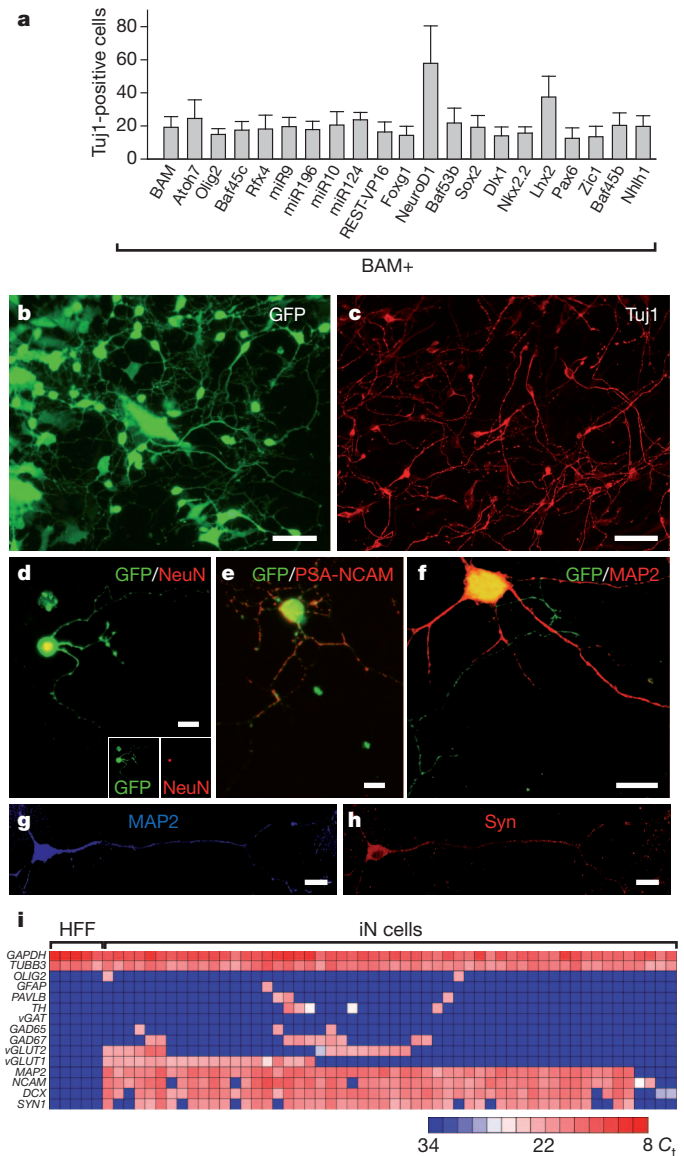


Figure 2 | NeuroD1 increases reprogramming efficiency in primary human fetal fibroblasts. **a**, Quantification of Tuj1-positive BAM-iN cells with indicated factors, 3 weeks after doxycycline treatment. **b**, **c**, Three weeks after doxycycline treatment BAM+NeuroD1 iN cells showed neuronal morphologies (**b**) and expressed Tuj1 (**c**). **d–f**, iN cells expressed NeuN (**d**), PSA-NCAM (**e**), and MAP2 (**f**) 2 weeks after doxycycline treatment. **g**, **h**, An iN cell expressing MAP2 (**g**) and synapsin (**h**) 4 weeks after doxycycline treatment and co-cultured with primary astrocytes. **i**, Single-cell gene expression profiling using Fluidigm dynamic arrays. Rows represent the evaluated genes and columns represent individual cells. Heat map (blue to red) represents the threshold C_t values as indicated. Data in (**a**) are presented as mean \pm s.d. Scale bars, 100 μ m (**b**, **c**) and 10 μ m (**d–h**).

expression levels over time even after doxycycline withdrawal (Supplementary Fig. 10). Similarly, HFF-iN cells could be maintained in the absence of doxycycline for 3 weeks (Supplementary Fig. 11).

We next asked whether iN cells generated from HFFs had active membrane properties. iN cells were identified by EGFP fluorescence (Fig. 3b) and whole-cell recordings were performed 14–35 days after doxycycline treatment. Two to three weeks after addition of doxycycline the average resting membrane potential of HFF-iN cells was -52.2 ± 2.2 mV (mean \pm s.e.m., $n = 41$). When HFF-iN cells were step-depolarized, action potentials could be detected in many iN cells at 14–25 days, and in all recorded iN cells at days 34–35 (Fig. 3c, Supplementary Figs 7 and 12 and Supplementary Table 1). Fast-activating and inactivating inward Na^+ currents as well as outward K^+ currents were also observed (Fig. 3d).

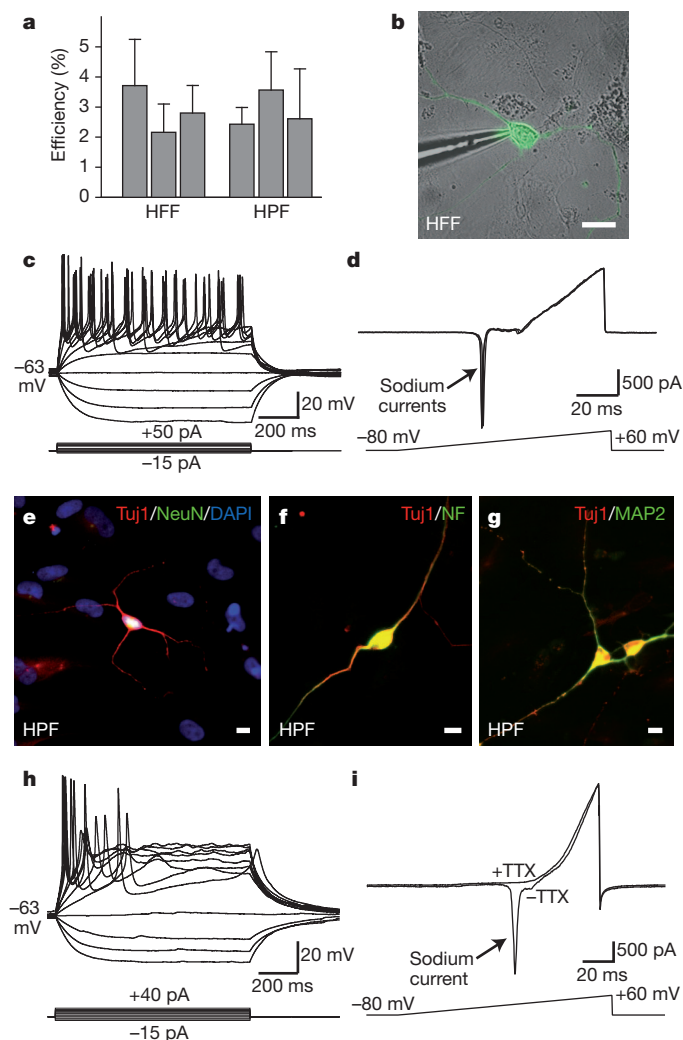


Figure 3 | Membrane properties of fibroblast iN cells. **a**, Quantification of Tuj1-positive neuronal cells from HFFs (line HFF-A) 3 weeks after doxycycline treatment or HPFs (line HPF-B) 4 weeks after doxycycline treatment. $n = 3$ independent experiments. **b**, Patch clamp recording was conducted on HFF-iN cells identified by EGFP fluorescence and differential interference contrast microscopy. **c**, Representative traces of membrane potentials in response to step current injections (lower panel) from an HFF-iN cell 19 days after doxycycline treatment. Membrane potential was maintained at approximately -63 mV. **d**, Representative traces of membrane currents recorded with a ramp protocol (lower panel). Fast activating and inactivating Na⁺ currents were prominent. Three traces are shown superimposed. **e-g**, HPF-iN cells express Tuj1 (red) and NeuN (green) (e), neurofilament (green, NF) (f) and MAP2 (green) (g). **h**, Representative traces of membrane potentials in response to step current injections in HPF-iN cells. Action potentials were generated in cultures without glia. **i**, Representative traces of membrane currents recorded following a ramp protocol (lower panel) in HPF-iN cells. The Na⁺ currents could be blocked by tetrodotoxin (TTX). Data in **a** are presented as mean \pm s.d. Scale bars, 10 μ m (a, e-g).

To determine whether the BAMN factors were also capable of converting more mature human fibroblasts into iN cells, we derived primary human postnatal fibroblasts (HPFs) from three different perinatal foreskin resections. In all three HPF lines, expression of BAMN factors reproducibly generated neuron-like cells with co-expression of multiple pan-neuronal markers (Fig. 3e-g). Intriguingly, the efficiencies of iN cell generation from fetal and postnatal fibroblasts were similar (2-4% of cells plated; Fig. 3a). Single-cell gene-expression profiling of iN cells revealed that 46 of 51 HPF iN cells co-expressed pan-neuronal and synaptic markers 42 days after infection; the majority of the HPF iN cells (37 of 51) seem to be glutamatergic neurons. Immunofluorescence analysis showed that 6 weeks after infection, $81 \pm 17\%$ of iN cells

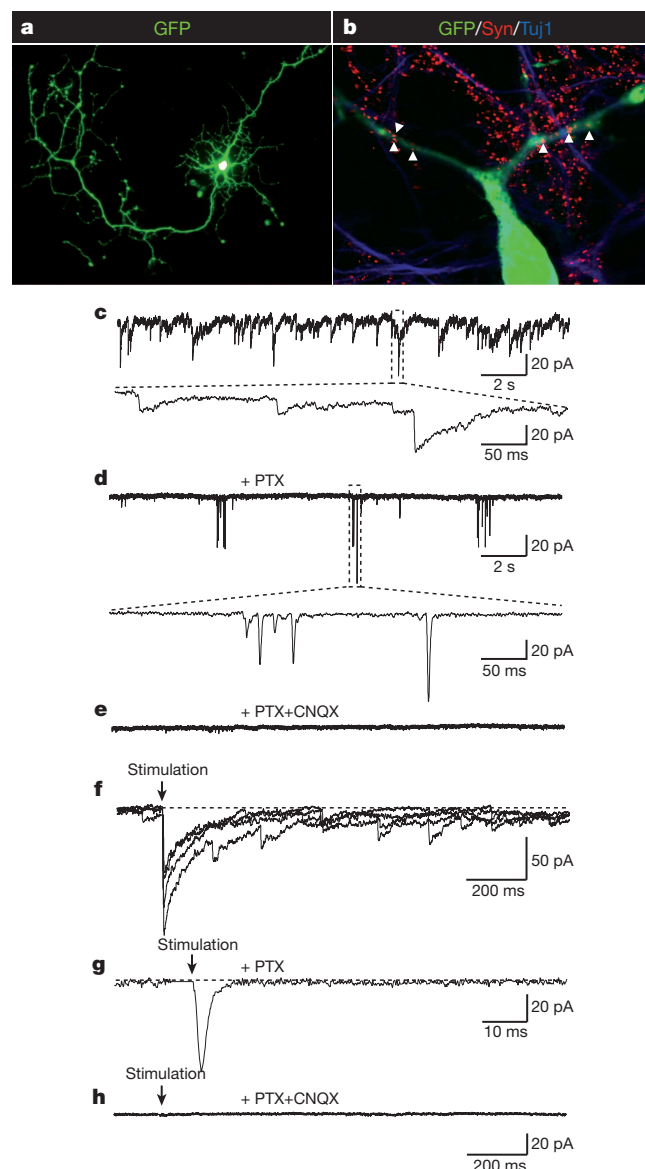


Figure 4 | Synaptic responses of HFF-iN cells. **a**, An HFF-iN cell expressing EGFP co-cultured with mouse cortical neurons at day 35 after doxycycline treatment. **b**, Synapsin-positive puncta co-localize with neurites extending from HFF-iN cells (arrow heads). **c**, Thirty-five days after doxycycline treatment, spontaneous PSCs were recorded in HFF-iN cells. **d**, Slow responses could be blocked by picrotoxin (PTX). The insert shows the fast kinetics of the responses. **e**, In the presence of PTX and CNQX (both 50 μ M), no spontaneous activities were observed. **f**, Evoked postsynaptic responses. Four traces were superimposed. **g**, In the presence of PTX, electric stimulation evoked fast-kinetic excitatory PSCs (EPSCs). **h**, No evoked synaptic responses were observed in the presence of PTX and CNQX. Scale bars, 100 μ m (a) and 10 μ m (b).

expressed Tbr1 above the levels of fibroblasts, and $15.2 \pm 6.6\%$ were peripherin-positive (Supplementary Fig. 13). Unlike fetal fibroblasts, most postnatal fibroblasts showed weak but specific Tbr1 staining (Supplementary Fig. 13a-d). Electrophysiological recordings demonstrated the presence of regenerative action potentials as well as voltage-dependent channel activities in the majority of cells analysed from two lines (for example, 17 of 18 cells from line HPF-B, Fig. 3h, i and Supplementary Table 1). Furthermore, iN cells with active membrane properties could be generated from dermal fibroblasts derived from an 11-year-old human subject (Supplementary Fig. 14).

Finally, we determined whether human iN cells can express functional neurotransmitter receptors and form functional synapses.

Application of either GABA (γ -aminobutyric acid) or L-glutamate to HFF-iN cells induced current responses that could be blocked by picrotoxin and CNQX, respectively (Supplementary Fig. 12e, f). We then dissociated HFFs 4–7 days after infection with the BAMN factors and EGFP and plated them onto previously established mouse cortical neuronal cultures. These co-cultures were maintained for up to 5 weeks thereafter. HFF-iN cells were identified by the EGFP expression (Fig. 4a). Whole-cell recordings after 2–3 weeks of co-culture showed no synaptic activity ($n = 20$) but after 4–5 weeks approximately half of human iN cells recorded showed spontaneous post-synaptic currents (PSCs) with variable kinetics ($n = 21$, Fig. 4c and Supplementary Table 1). Immunostaining with synapsin antibodies confirmed the presence of scattered synaptic puncta on the dendrites of EGFP-positive cells (Fig. 4b). When the GABA_A receptor inhibitor picrotoxin was applied, the majority of the spontaneous PSCs were blocked, demonstrating that they were inhibitory (IPSCs) (Fig. 4d). In the presence of picrotoxin, bursting of spontaneous excitatory post-synaptic currents (EPSCs) was shown and could be blocked by the AMPA (α -amino-3-hydroxy-5-methyl-4-isoxazole propionic acid) receptor blocker CNQX (Fig. 4e). Focal stimulation evoked both IPSCs and EPSCs that could be blocked by picrotoxin and CNQX (Fig. 4f–h). Importantly, PSCs could also be recorded from HPF-iN cells co-cultured with mouse cortical neurons 4 weeks after infection (Supplementary Fig. 15). These results demonstrate that fetal and postnatal fibroblast-derived iN cells could form functional synapses and integrated into pre-existing neuronal networks.

In this report, we have identified a combination of transcription factors that are capable of converting human fibroblasts directly into neurons. Like mouse iN cells¹³ and neurons derived from ES cells^{19–21} and iPS cells^{22,23}, the human iN cells seem relatively immature, as indicated by their slightly depolarized membrane potentials and the relatively low-amplitude synaptic responses. Compared to mouse iN cells, human iN cells required longer culture periods to develop synaptic activity. Future studies will be necessary to thoroughly optimize conditions for human iN cell generation and maturation, which would facilitate applications of this method for the study of human neuronal development and disease.

METHODS SUMMARY

Cell culture. H9 human ES cells (WiCell Research Resources) and iPS cells were expanded in mTeSR1 (Stem Cell Technologies) and passaged as clumps or single cells²⁴. Primary HFFs were isolated from the distal half of the limbs of GW8-10 fetuses obtained from Advanced Bioscience Resources Inc. Primary HPFs were established from foreskin. Primary mouse cortical cultures and glial monolayer cultures were established as described previously¹³.

Lentiviral infections. Lentiviral production and fibroblast infections were performed as described previously¹³. Primary fibroblasts and pluripotent stem cells were infected with concentrated lentivirus and treated with doxycycline ($2 \mu\text{g} \mu\text{l}^{-1}$) 16–24 h later.

Electrophysiology and expression analysis. Cells were analysed by immunofluorescence and electrophysiology as described elsewhere^{13,25}. Single-cell gene expression profiling was performed using the Fluidigm Biomark dynamic array^{18,26} according to the manufacturer's instructions.

Full Methods and any associated references are available in the online version of the paper at www.nature.com/nature.

Received 1 November 2010; accepted 18 May 2011.

Published online 26 May 2011.

- Blau, H. M. *et al.* Plasticity of the differentiated state. *Science* **230**, 758–766 (1985).
- Gurdon, J. B. From nuclear transfer to nuclear reprogramming: the reversal of cell differentiation. *Annu. Rev. Cell Dev. Biol.* **22**, 1–22 (2006).
- Heins, N. *et al.* Glial cells generate neurons: the role of the transcription factor Pax6. *Nature Neurosci.* **5**, 308–315 (2002).
- Ieda, M. *et al.* Direct reprogramming of fibroblasts into functional cardiomyocytes by defined factors. *Cell* **142**, 375–386 (2010).

- Shen, C.-N., Slack, J. M. W. & Tosh, D. Molecular basis of transdifferentiation of pancreas to liver. *Nature Cell Biol.* **2**, 879–887 (2000).
- Tada, M., Takahama, Y., Abe, K., Nakatsuji, N. & Tada, T. Nuclear reprogramming of somatic cells by *in vitro* hybridization with ES cells. *Curr. Biol.* **11**, 1553–1558 (2001).
- Takahashi, K. *et al.* Induction of pluripotent stem cells from adult human fibroblasts by defined factors. *Cell* **131**, 861–872 (2007).
- Wilmut, I., Schnieke, A. E., McWhir, J., Kind, A. J. & Campbell, K. H. Viable offspring derived from fetal and adult mammalian cells. *Nature* **385**, 810–813 (1997).
- Xie, H., Ye, M., Feng, R. & Graf, T. Stepwise reprogramming of B cells into macrophages. *Cell* **117**, 663–676 (2004).
- Zhou, Q., Brown, J., Kanarek, A., Rajagopal, J. & Melton, D. A. *In vivo* reprogramming of adult pancreatic exocrine cells to β -cells. *Nature* **455**, 627–632 (2008).
- Graf, T. & Enver, T. Forcing cells to change lineages. *Nature* **462**, 587–594 (2009).
- Zhou, Q. & Melton, D. A. Extreme makeover: converting one cell into another. *Cell Stem Cell* **3**, 382–388 (2008).
- Vierbuchen, T. *et al.* Direct conversion of fibroblasts to functional neurons by defined factors. *Nature* **463**, 1035–1041 (2010).
- Hansen, D. V., Lui, J. H., Parker, P. R. & Kriegstein, A. R. Neurogenic radial glia in the outer subventricular zone of human neocortex. *Nature* **464**, 554–561 (2010).
- Kriegstein, A., Noctor, S. & Martinez-Cerdeno, V. Patterns of neural stem and progenitor cell division may underlie evolutionary cortical expansion. *Nature Rev. Neurosci.* **7**, 883–890 (2006).
- Zhang, X. *et al.* Pax6 is a human neuroectoderm cell fate determinant. *Cell Stem Cell* **7**, 90–100 (2010).
- Bottenstein, J. E. & Sato, G. H. Growth of a rat neuroblastoma cell line in serum-free supplemented medium. *Proc. Natl Acad. Sci. USA* **76**, 514–517 (1979).
- Guo, G. *et al.* Resolution of cell fate decisions revealed by single-cell gene expression analysis from zygote to blastocyst. *Dev. Cell* **18**, 675–685 (2010).
- Johnson, M. A., Weick, J. P., Pearce, R. A. & Zhang, S. C. Functional neural development from human embryonic stem cells: accelerated synaptic activity via astrocyte coculture. *J. Neurosci.* **27**, 3069–3077 (2007).
- Wu, H. *et al.* Integrative genomic and functional analyses reveal neuronal subtype differentiation bias in human embryonic stem cell lines. *Proc. Natl Acad. Sci. USA* **104**, 13821–13826 (2007).
- Koch, P., Opitz, T., Steinbeck, J. A., Ladewig, J. & Brustle, O. A rosette-type, self-renewing human ES cell-derived neural stem cell with potential for *in vitro* instruction and synaptic integration. *Proc. Natl Acad. Sci. USA* **106**, 3225–3230 (2009).
- Marchetto, M. C. *et al.* A model for neural development and treatment of Rett syndrome using human induced pluripotent stem cells. *Cell* **143**, 527–539 (2010).
- Hu, B. Y. *et al.* Neural differentiation of human induced pluripotent stem cells follows developmental principles but with variable potency. *Proc. Natl Acad. Sci. USA* **107**, 4335–4340 (2010).
- Xu, Y. *et al.* Revealing a core signaling regulatory mechanism for pluripotent stem cell survival and self-renewal by small molecules. *Proc. Natl Acad. Sci. USA* **107**, 8129–8134 (2010).
- Maximov, A., Pang, Z. P., Tervo, D. G. & Sudhof, T. C. Monitoring synaptic transmission in primary neuronal cultures using local extracellular stimulation. *J. Neurosci. Methods* **161**, 75–87 (2007).
- Wong, C. C. *et al.* Non-invasive imaging of human embryos before embryonic genome activation predicts development to the blastocyst stage. *Nature Biotechnol.* **28**, 1115–1121 (2010).

Supplementary Information is linked to the online version of the paper at www.nature.com/nature.

Acknowledgements We would like to thank Y. Kokubu for technical assistance in molecular cloning and Y. Zhang for assistance in iPS cell induced neuron culture. We also thank Y. Sun for providing the microRNAs expression lentiviral vectors and S. Majumder for the REST-VP16 construct. This work was enabled by start-up funds from the Institute for Stem Cell Biology and Regenerative Medicine at Stanford (M.W.), the Ellison Medical Foundation (M.W.), the Stinehard-Reed Foundation (M.W.), the Donald E. and Delia B. Baxter Foundation (M.W.), the NIH grants 1R01MH092931 (M.W. and T.C.S.) and RC4 NS073015 (M.W.), and a Robertson Investigator Award from the New York Stem Cell Foundation. Z.P.P. is supported by 2008 and 2010 NARSAD Young Investigator Awards. T.V. is supported by the Ruth and Robert Halperin Stanford Graduate Fellowship. A.C. is supported by the AXA research fund and D.R.F. is supported by BioX Undergraduate Fellowship.

Author Contributions Z.P.P., N.Y., T.V., A.O., T.C.S. and M.W. designed the experiments and analysed the data. D.R.F. and T.Q.Y. helped with lentiviral production. A.C., V.S. and S.M. helped to provide experimental material and helped with the analyses. Z.P.P., N.Y., T.V., T.C.S. and M.W. wrote the paper.

Author Information Reprints and permissions information is available at www.nature.com/reprints. The authors declare no competing financial interests. Readers are welcome to comment on the online version of this article at www.nature.com/nature. Correspondence and requests for materials should be addressed to M.W. (wernig@stanford.edu).

METHODS

Cell culture. H9 human ES cells (WiCell Research Resources) were expanded in mTeSR1 (Stem Cell Technologies). Induced pluripotent stem cells were generated as described elsewhere²⁷. The day before infection, cells were treated with Accutase and seeded as single cells in 3.5-cm tissue culture dishes on Matrigel in mTeSR1 containing 2 μ M thiazovivin (Bio Vision)²⁴. To inhibit the growth of uninfected ES cells and select for post-mitotic neurons, we added 4 μ M cytosine β -D-arabinofuranoside (Ara-C) to the media 48 h after doxycycline addition. Primary human fetal fibroblasts were isolated from the distal half of the limbs of 8–10-week-old fetuses (Advanced Bioscience Resources Inc.). The tissue was dissociated after trypsin digestion and plated in MEF media (DMEM high glucose, calf serum, sodium pyruvate, non-essential amino acids, penicillin/streptomycin and β -mercaptoethanol). Primary human postnatal fibroblasts (HPFs) were established from dissociated foreskin tissue derived from 1–3-day-old newborns. Before being used for experiments, primary fibroblast cells were passaged at least three times. Primary mouse cortical cultures and glial monolayer cultures were established as described previously¹³. To maintain the iN cell culture, cells were either grown in N3 medium (DMEM/F2 (Invitrogen), apotransferrin (100 μ g ml⁻¹), insulin (5 μ g ml⁻¹), sodium selenite (30 nM), progesterone (20 nM), putrescine (100 nM), penicillin/streptomycin) supplemented with neurotrophic factors including brain-derived neurotrophic factor, glial-cell-derived neurotrophic factor, neurotrophin-3 and ciliary neurotrophic factor (R&D systems), or dissociated using papain and replated onto previously established monolayer culture of primary mouse glia or primary neurons from mouse cortex in neuronal growth medium (MEM (Gibco) supplemented with B27 (Gibco), glucose (5 mg ml⁻¹), transferring (10 μ g ml⁻¹), 5% fetal bovine serum and Ara-C (2 μ M, Sigma)^{13,25}.

Virus infections. Lentiviral production and fibroblast infections were performed as described previously¹³. Briefly, primary human fetal or postnatal fibroblasts were plated and infected with concentrated lentiviral particles and polybrene (8 μ g μ l⁻¹) in fresh MEF medium. Viral medium was removed after 16–24 h and replaced with MEF medium containing doxycycline (2 μ g μ l⁻¹). After 24–48 h, medium was changed to N3 medium containing doxycycline (2 μ g μ l⁻¹). For human ES cell infections, H9 human embryonic stem cells were switched into N3 medium containing polybrene (2 μ g μ l⁻¹) 24 h after re-plating, and concentrated lentiviral particles were added. After 16–24 h, cultures were switched to N3 medium containing doxycycline (2 μ g μ l⁻¹) and changed daily before dissociation. Forty-eight hours after the initial addition of doxycycline, Ara-C (4 μ g μ l⁻¹) was added to the medium to inhibit proliferation of uninfected ES cells until analysis 6 days after the addition of doxycycline. All chemicals were purchased from Sigma-Aldrich if not otherwise specified.

Single-cell gene expression analysis (Fluidigm dynamic array). Single-cell gene expression profiling was performed using the Fluidigm Biomark dynamic array according to the manufacturer's protocol^{18,26}. Briefly, single cells growing on culture dishes after 5 or 6 weeks of transduction were collected by aspiration into patch electrodes and ejected into 2 \times cellsdirect buffer (Invitrogen), flash-frozen and kept at -80°C until further processing. Thawed cells were subject to target-specific reverse-transcription and 18 cycles of PCR pre-amplification with a mix of primers specific to the target genes (STA). STA products were then processed for real-time PCR analysis on Biomark 48:48 Dynamic Array integrated fluidic circuits (Fluidigm). To ensure the specificity of the amplification, titrations of total human brain RNA were included in each experiment, and only primers that demonstrated a linear amplification were analysed. Furthermore, melting curves of the PCR products were compared between the single cells and the control RNA to ensure the specificity of the PCR products.

Electrophysiology. Action potentials were recorded with current-clamp whole-cell configuration. The pipette solution for current-clamp experiments contained (in mM): 123 K-gluconate, 10 KCl, 1 MgCl₂, 10 HEPES, 1 EGTA, 0.1 CaCl₂, 1 K₂ATP, 0.2 Na₄GTP and 4 glucose, pH adjusted to 7.2 with KOH. Membrane potentials were kept around -65 to -70 mV, and step currents were injected to elicit action potentials. For whole-cell voltage-dependent current recordings, the same internal solution as aforementioned was used. For synaptic functional evaluation, the internal solution contained (in mM): 135 CsCl, 10 HEPES, 1 EGTA, 4 Mg-ATP, 0.4 Na₄GTP, and 10 QX-314, pH 7.4. The bath solution contained (in mM): 140 NaCl, 5 KCl, 2 CaCl₂, 2 MgCl₂, 10 HEPES, and 10 glucose, pH 7.4. Synaptic responses were measured as described previously^{13,25}. Stimulus artefacts for evoked synaptic responses were removed for graphic representation. Electrophysiological data are presented as mean \pm s.e.m. All statistical comparisons were made using Student's *t*-test.

Immunofluorescence and RT-PCR. For immunofluorescence experiments, cells were fixed in 4% paraformaldehyde in PBS for 10 min at room temperature. After fixation, cells were incubated in 0.2% Triton X-100 in PBS for 5 min at room temperature. After washing twice with PBS, cells were blocked in a solution of PBS containing 4% BSA and 1% Cosmic calf serum (CCS) for 30 min at room temperature. Primary and secondary antibodies were applied for 1 h and 30 min, respectively. The following antibodies were used for our analysis: rabbit anti-Tuj1 (Covance, 1:1,000), mouse anti-Tuj1 (Covance, 1:1,000), mouse anti-MAP2 (Sigma, 1:500), mouse anti-NeuN (Millipore, 1:200), mouse anti-neurofilament (Developmental Studies Hybridoma Bank (DSHB), 2H3a, 1:1,000), rabbit anti-synapsin (E028, 1:1,000), anti-synaptotagmin (Synaptic systems, 41.1, 1:2,000), guinea pig anti-vGLUT1 (Millipore, 1:2,000), mouse anti-GAD6 (DSHB, 1:500), rabbit anti-Tbr1 (Abcam, 1:200), mouse anti-peripherin (Sigma, 1:100), sheep anti-tyrosine hydroxylase (Pel-Freez, 1:500), rabbit anti-GFAP (DAKO, 1:4,000), mouse anti-Sox2 (R&D Systems, 1:50), goat anti-Brn2 (clone C-20, Santa Cruz Biotechnology, 1:100), rabbit anti-Ascl1 (Abcam, 1:200), mouse anti-BrdU (Becton Dickinson, 1:50), mouse anti-LU5 (Abcam, 1:200), goat anti-Sox10 (Santa Cruz Biotechnology, 1:40). Fluorescein isothiocyanate (FITC)-, and Cy3-conjugated secondary antibodies were obtained from Jackson ImmunoResearch. Alexa-488-, Alexa-546- and Alexa-633-conjugated secondary antibodies were obtained from Invitrogen. 4',6-Diamidino-2-phenylindole (DAPI) was from Sigma (1:10,000). For RT-PCR analysis, RNA was isolated using an RNAqueous Kit (Applied Biosystems) following the manufacturer's instructions, treated with DNase (Applied Biosystems) and reverse-transcribed with Superscript III (Invitrogen).

Efficiency calculation. The following method was used to calculate the efficiency of neuronal induction. The total number of Tuj1-positive cells with a neuronal morphology, defined as cells having a circular, three-dimensional appearance that extend a thin process at least three times longer than their cell body, were quantified at indicated time points. We determined this number in at least 15 randomly selected $\times 20$ visual fields on a Zeiss Axio Observer microscope. The average and standard deviation per field was determined and then used to extrapolate the total number of iN cells present in the entire dish based the known surface areas of a $\times 20$ visual field and the respective culture dish. We then divided this number by the number of cells plated before infection to get the percentage of the starting population of cells that adopted neuron-like characteristics. In multiple independent experiments we verified that this extrapolation method yields cell numbers very similar to those measured by a haemocytometer at the time of plating. Data are presented as mean \pm s.d.

27. Somers, A. *et al.* Generation of transgene-free lung disease-specific human induced pluripotent stem cells using a single excisable lentiviral stem cell cassette. *Stem Cells* **28**, 1728–1740 (2010).